

# Reexamination of Finite-Lattice Extrapolation of Haldane Gaps

Hiroki NAKANO \* and Akira TERAI<sup>1</sup> †

*Graduate School of Material Science, University of Hyogo, Kouto 3-2-1, Kamiori, Ako-gun, 678-1297*

<sup>1</sup>*Department of Applied Physics, Osaka City University, Sumiyoshi-ku, Osaka 558-8585*

(Received October 26, 2018)

We propose two methods of estimating a systematic error in extrapolation to the infinite-size limit in the study of measuring the Haldane gaps of the one-dimensional Heisenberg antiferromagnet with the integer spin up to  $S = 5$ . The finite-size gaps obtained by numerical diagonalizations based on Lanczos algorithm are presented for sizes that have not previously been reported. The changes of boundary conditions are also examined. We successfully demonstrate that our methods of extrapolation work well. The Haldane gap for  $S = 1$  is estimated to be  $0.4104789 \pm 0.0000013$ . We successfully obtain the gaps up to  $S = 5$ , which make us confirm the asymptotic formula of the Haldane gap in  $S \rightarrow \infty$ .

KEYWORDS: Antiferromagnetic Heisenberg spin chain, Haldane gap, Exact-diagonalization method, Lanczos method, Extrapolation

## 1. Introduction

Extrapolation is a fundamental technique in a lot of studies in physics. In particular, the technique is often carried out in the condensed-matter physics when one attempts to know a quantity in the thermodynamic limit from several finite-size data. One of the reliable ways to obtain such finite-size data is the numerical-diagonalization method applied to the Hamiltonian matrix describing a system. This method provides us with very precise finite-size data although available system sizes are limited to being very small. This method is non-biased against the effects of interaction; thus it contributes much to the understanding of many-body problems. Typical examples are the quantum spin systems, in which there often appear nontrivial quantum states due to the presence of interactions between spins. One of them is the ground state of the integer-spin one-dimensional Heisenberg antiferromagnet. In this system, an energy gap exists between the unique ground state and the first excited state; this gap is called the Haldane gap.<sup>1,2</sup>

The magnitude of the Haldane gap has been estimated by various numerical methods.<sup>3</sup> There are three representative approaches. The first one is the numerical Lanczos diagonalization of finite-size clusters. In the  $S = 1$  case, system sizes up to 22 sites were treated under the periodic boundary condition.<sup>4</sup> Since the available system sizes are small, an appropriate extrapolation is required. Unfortunately, it is difficult to estimate a systematic error due to the extrapolation. The second one is the density matrix renormalization group (DMRG) method.<sup>5</sup> The calculation was carried out under a peculiar boundary condition, namely, each edge of the  $S = 1$  chain connecting with an  $S = 1/2$  spin. In this way, it is necessary to tune the artificial interaction at the edges. The third one is a quantum Monte Carlo (QMC) simulation.<sup>6</sup> Since this simulation was performed by the loop algorithm together with a continuous imaginary time technique, cal-

culations of very large systems are available. However, a statistical error due to a Monte Carlo sampling cannot be avoided. Up to the present time, these approaches give consistent estimates of the Haldane gap with their own errors of the same order.

Under such circumstances, we attempt again to estimate the Haldane gaps of the Heisenberg antiferromagnetic spin chain as precisely as possible. Our main method is the numerical diagonalization. A primary purpose of this paper is to propose a procedure to obtain a reliable error in extrapolation of finite-size data toward the infinite size of the system.

In the extrapolation, the weak system-size dependence of the finite-size gap is favored. The system-size dependence of the gap is determined by the choice of the boundary condition. It is known that the dependence becomes suppressed when one twists the boundary condition from the periodic boundary condition.<sup>7</sup> Under this background, we examine boundary conditions in the case of  $S = 1$  to know which boundary condition is appropriate. We then find that the twisted boundary condition is the most appropriate one among periodic, twisted, and open boundary conditions. The twisted boundary condition gives a good sequence of finite-size excitation gaps for the sake of the extrapolation. Next, we develop a method to obtain a reliable error when the convergence of the data sequence can be accelerated. Thereby, a very precise estimation of the  $S = 1$  Haldane gap is successfully obtained. When one imposes the twisted boundary condition for  $S = 2, 3, 4$ , and  $5$ , the Haldane gaps can be obtained to be nonzero values in the thermodynamic limit in spite of the fact that the Lanczos method can treat only the extremely small system sizes. When  $S$  becomes larger, the convergence acceleration becomes more difficult. In such a case of the acceleration in failure, we also develop another procedure to estimate an error to the excitation gap of the infinite system.

This paper is organized as follows. In the next section, the model Hamiltonian and the method of calculation will be explained. In the first half of §3, the numerical

\*E-mail address: hnakano@sci.u-hyogo.ac.jp

†E-mail address: terai@a-phys.eng.osaka-cu.ac.jp

results of the  $S = 1$  system are presented and discussed. Boundary conditions are examined and the extrapolation based on the convergence acceleration is performed. We propose its error estimation and demonstrate the validity. In the second half of §3, the cases of  $S \geq 2$  are studied. Another procedure of obtaining an error is introduced. The final section is devoted to the summary and some remarks.

## 2. Hamiltonian and Method

The Hamiltonian of the present model is given by

$$\mathcal{H} = \sum_{i=1}^N J_m \mathbf{S}_m \cdot \mathbf{S}_{m+1}, \quad (1)$$

where  $\mathbf{S}_m$  is a spin operator with its amplitude  $S$  at site  $m$ . Here  $N$  is the number of spin sites. The system size  $N$  is supposed to be an even integer. The amplitude of the exchange interaction is denoted by  $J_m$  which will be defined later when the boundary conditions is explained.

In this paper, we carry out numerical diagonalizations for finite-size clusters of systems of  $S = 1, 2, 3, 4$ , and  $5$ . We calculate the ground-state energy  $E_0$  and excitation energies (the first excitation  $E_1$  and the second excitation  $E_2$ ) by the method of Lanczos algorithm.<sup>8</sup> We have successfully developed a code for parallel calculations of the Lanczos algorithm. The maximum sizes in this paper are  $N = 24$  for  $S = 1$ ,  $N = 16$  for  $S = 2$ ,  $N = 12$  for  $S = 3$ ,  $N = 12$  for  $S = 4$ , and  $N = 10$  for  $S = 5$ . These sizes have not been treated in the Lanczos calculations as long as the present authors know. Note that we only assume the conservation of the  $z$ -component of the total spin. Thus, arbitrary shapes of clusters can be treated. The dimensions of the Hilbert space are very large. For example, the dimension of the largest subspace, namely  $S_{\text{tot}}^z = 0$ , of  $N = 24$  for  $S = 1$  is 27 948 336 381, where  $S_{\text{tot}}^z$  is the  $z$  component of the total spin. It is worth to emphasize that the parallelization makes it possible to carry out the Lanczos calculations.

## 3. Result and Discussion

### 3.1 Case for $S = 1$

#### 3.1.1 Boundary Conditions

Let us consider differences from the choice of boundary conditions. The differences from boundary conditions appear in results of calculations of finite-size systems. On the other hand, the differences are supposed to disappear in the limit of  $N \rightarrow \infty$ . Finite-size effects depend on the choice of a boundary condition. Namely, a different type of boundary condition gives a different finite-size sequence concerning with a physical quantity. In order to obtain precisely the information in the thermodynamic limit that is not affected by boundary conditions, one should employ an appropriate boundary condition. Such a condition is not necessarily the periodic boundary condition. The appropriate condition depends on systems and physical quantities. Therefore, the examination of various boundary conditions is important. Here we focus our attention on the problem of the Haldane gaps and begin with such an examination in the  $S = 1$  case.

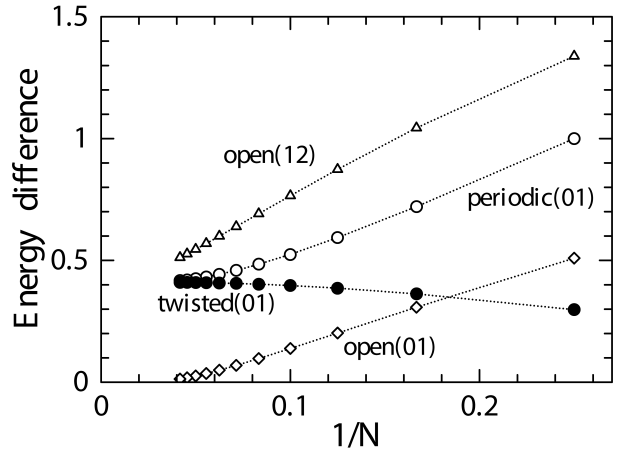


Fig. 1. Energy differences of finite-size  $S = 1$  systems. Open and closed circles denote results of  $E_1 - E_0$  under the periodic boundary condition and the twisted boundary condition, respectively. Triangles and diamonds denote results of  $E_2 - E_1$  and  $E_1 - E_0$  under the open boundary condition, respectively. Note that the maximum system size is  $N = 24$  irrespective of boundary conditions.

In this paper, we examine three types of the boundary conditions: the open, periodic, and twisted boundary conditions. The open boundary condition is given by

$$J_m = \begin{cases} 1 & (m < N) \\ 0 & (m = N). \end{cases} \quad (2)$$

The periodic boundary condition is given by  $\mathbf{S}_{N+1} = \mathbf{S}_1$  and  $J_m = 1$  for arbitrary  $m$ . The twisted boundary condition is given by

$$S_{N+1}^x = -S_1^x, \quad S_{N+1}^y = -S_1^y, \quad S_{N+1}^z = S_1^z, \quad (3)$$

and  $J_m = 1$  for arbitrary  $m$ . Note here that energies are measured in units of nonzero  $J_m$ ; therefore we take it unity.

First, we show numerical results of system size dependence of energy differences in Fig. 1. Our results under the periodic boundary condition agree with those in ref. 4 up to  $N = 22$ ; our results for  $N = 24$  are new. One can clearly observe that  $E_1 - E_0$  under the open boundary condition vanishes in the limit of  $N \rightarrow \infty$ . This behavior is consistent with a quasi-degeneracy of the Haldane-type ground states. Under the open boundary condition, the Haldane gap appears above these degenerate ground states; the energy difference  $E_2 - E_1$  decreases gradually when  $N$  is increased and seems to converge around 0.4. Under the twisted boundary condition, on the other hand, the energy difference  $E_1 - E_0$  increases with increasing  $N$ . This dependence will also be very useful when we study gaps for the cases of  $S \geq 2$ . In this section, let us compare the speed of the convergence of the finite-size sequence under each boundary condition. In order to achieve it, we consider the ratio defined as

$$R^{\zeta}(N, m) = \frac{G^{\zeta}(N) - G^{\zeta}(N + m)}{G^{\zeta}(N) - G^{\zeta}(N + m)}. \quad (4)$$

Here  $G^{\zeta}(N)$  is the energy difference with system size  $N$  under the  $\zeta$  boundary condition which converges to the Haldane gap in the limit of  $N \rightarrow \infty$ ; namely,  $G^{\zeta}(N) =$

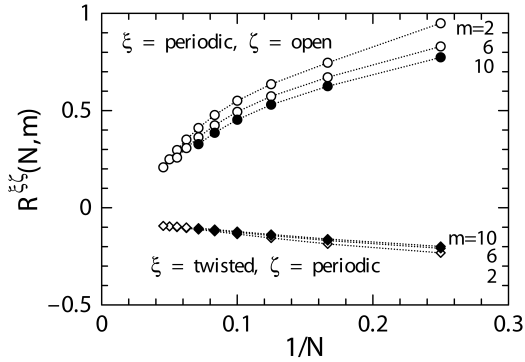


Fig. 2. Ratio  $R^{\xi\zeta}(N, m)$  v.s. inversed system sizes. Circles denote the case of  $\xi = \text{periodic}, \zeta = \text{open}$ . Diamonds denote the case of  $\xi = \text{twisted}, \zeta = \text{periodic}$ . Closed symbols mean  $m = 10$  which is the largest  $m$  in this figure.

$E_1 - E_0$  for the periodic and twisted boundary conditions, and  $G^{\zeta=\text{open}}(N) = E_2 - E_1$ . Results of the ratio  $R^{\xi\zeta}(N, m)$  v.s.  $1/N$  are depicted for two types in Fig. 2. All the absolute values of the presented ratios are less than unity. The ratio of  $\xi = \text{periodic}$  and  $\zeta = \text{open}$  gets gradually smaller when  $N$  is increased. The ratio seems to vanish in the limit of  $N \rightarrow \infty$ . If the ratio in the limit of  $m \rightarrow \infty$  vanishes and when each  $G^\zeta(N)$  converges to the same value, namely the Haldane gap  $\Delta(S = 1)$  in this case, one obtains

$$\lim_{N \rightarrow \infty} \frac{G^\xi(N) - \Delta(S = 1)}{G^\zeta(N) - \Delta(S = 1)} = 0. \quad (5)$$

This suggests that the sequence under the periodic boundary condition converges faster than that under the open boundary condition. (See appendix.) Thus the periodic boundary condition is more appropriate than the open boundary condition to measure the Haldane gap within the system sizes that are available in numerical diagonalization calculations. On the other hand, the ratio of  $\xi = \text{twisted}$  and  $\zeta = \text{periodic}$  in the limit of  $N \rightarrow \infty$  seems not to vanish but to converge to a nonzero value. This means that concerning with the convergence of the sequence, the speeds of cases of the twisted and periodic boundary conditions are almost the same with each other. Even though the speeds are comparable, the absolute values of the ratios are much smaller than unity ( $|R^{\xi\zeta}(N, m)| < 1/4$ ). This suggests that each datum of the sequence under the twisted boundary condition is closer to the Haldane gap  $\Delta(S = 1)$  than the corresponding datum under the periodic boundary condition. In this meaning, we can conclude that the twisted boundary condition is more appropriate than the periodic boundary condition. Therefore, the twisted boundary condition is the most appropriate among the present three conditions.

### 3.1.2 Extrapolation

In this subsection, we attempt to extrapolate the above sequences of the  $S = 1$  finite-size energy differences by means of the technique of convergence acceleration. We

here apply Wynn's epsilon algorithm<sup>9</sup> given by

$$\frac{1}{A_N^{(k+1)} - A_{N-2}^{(k)}} = \frac{1}{A_{N-4}^{(k)} - A_{N-2}^{(k)}} + \frac{1}{A_N^{(k)} - A_{N-2}^{(k)}} - \frac{\alpha}{A_{N-4}^{(k-1)} - A_{N-2}^{(k)}}, \quad (6)$$

when  $\alpha = 1$ . Here the initial condition is given by  $A_N^{(0)} = G(N)$  and  $A_N^{(-1)} = \infty$ . It was in ref. 4 that this transformation was applied for the first time to estimate the  $S = 1$  Haldane gap. Note that when we take  $\alpha = 0$  in eq. (6), the transformation is reduced to the one called as the Aitken-Shanks process.<sup>10</sup> The Aitken-Shanks transformation was used in ref. 11. Both of the transformations make us possible to accelerate the convergence of a finite sequence and to give a candidate for the extrapolated value. It is, however, difficult to obtain a systematic error only within the framework of each transformation. Under such circumstances, the authors of ref. 4 considered the variance of  $\alpha$  within a successful acceleration of the convergence. We have found problems in the argument of estimating their systematic error in ref. 4 when we examine the convergence of the  $S = 1$  finite-size gaps up to  $N = 24$  under the periodic boundary condition. We present the results of the table of the convergence for  $\alpha = 1$  in Table I. Note here that a part up to  $N = 22$  in Table I was reported and that the energy difference of  $N = 24$  and its posterity are new. Let us mention the problems while we are reviewing the procedure of ref. 4.

Let us explain the procedure of ref. 4 briefly. First, one considers the following decay lengths defined as

$$\xi_N^{(k)} = 2 / \log \left( \frac{A_{N-4}^{(k)} - A_{N-2}^{(k)}}{A_{N-2}^{(k)} - A_N^{(k)}} \right), \quad (7)$$

in order to examine converging behavior of the sequence  $A_N^{(k)}$  for each step  $k$ . One should note that  $\xi_N^{(0)}$  increases monotonically. This means that the convergence becomes slower when  $N$  is getting larger. This is a source of difficulties in estimating the extrapolated gap. In order to overcome this difficulty, an acceleration is introduced. To examine whether the acceleration of  $A_N^{(k)}$  for each  $k$  from  $A_N^{(k-1)}$  is successful or not, ref. 4 investigates the following three conditions.

- I**  $A_N^{(k)}$  for each  $k$  is monotonic.
- II**  $\xi_N^{(k)}$  for each  $k$  is monotonically increasing, namely, the following condition holds,

$$\xi_{N+2}^{(k)} > \xi_N^{(k)}. \quad (8)$$

- III** The following condition holds,

$$\xi_N^{(k+1)} < \xi_N^{(k)}. \quad (9)$$

Conditions **I** and **II** suggest that properties of the initial sequence are preserved even though the acceleration is carried out. Condition **III** means whether an element with a long decay length is successfully removed by the acceleration. ref. 4 considered that  $A_{N=22}^{(5)} = 0.410498$  is successfully accelerated and that it is reliable as an

Table I. Sequence of finite-size gaps for the  $S = 1$  case under the periodic boundary condition and the convergence acceleration based on Wynn's algorithm (eq.(6) with  $\alpha = 1$ ).

$N$	$G(N) = A_N^{(0)}$	$\xi_N^{(0)}$	$A_N^{(1)}$	$\xi_N^{(1)}$	$A_N^{(2)}$	$\xi_N^{(2)}$	$A_N^{(3)}$	$\xi_N^{(3)}$	$A_N^{(4)}$	$\xi_N^{(4)}$	$A_N^{(5)}$
2	2										
4	1										
6	0.720627362624	1.57	0.61232025								
8	0.593555254375	2.54	0.48753251								
10	0.524807950414	3.26	0.44377567	1.91	0.43525877						
12	0.484196469912	3.80	0.42557752	2.28	0.41798489						
14	0.458965346938	4.20	0.41757427	2.43	0.41308940	1.59	0.41258393				
16	0.442795561359	4.50	0.41394088	2.53	0.41152416	1.75	0.41114647				
18	0.432221469865	4.71	0.41223978	2.64	0.41095437	1.98	0.41074380	1.57	0.41071215		
20	0.425210314459	4.87	0.41141374	2.77	0.41071416	2.32	0.41058977	2.08	0.41055478		
22	0.420515020390	4.99	0.41099554	2.94	0.41059985	2.69	0.41052336	2.38	0.41050133	1.85	0.41049811
24	0.417346883838	5.08	0.41077448	3.14	0.41054158	2.97	0.41049612	2.24	0.41048618	1.59	0.41048426

approximate for the gap value. In ref. 4, the region of  $\alpha$  where all the three conditions hold was found around  $\alpha = 1$  within data up to  $N = 22$  even when one applies the acceleration iteratively up to  $k = 5$ . Finally, the obtained region of  $\alpha$  gave a systematic error.

Let us examine the situations in all the presently available data up to  $N = 24$ . In Table I,  $\xi_N^{(k)}$  up to  $k = 2$  are monotonically increasing. However, one finds that  $\xi_N^{(3)}$  does not show a monotonic  $N$ -dependence and that  $\xi_N^{(4)}$  decreases with  $N$ . Condition (8) does not hold. This means that it is unclear whether the acceleration of  $A_N^{(3)}$ ,  $A_N^{(4)}$ , and  $A_N^{(5)}$  are successful or not. Next, we examine the behavior of  $\xi_N^{(3)}$  and  $\xi_N^{(4)}$  when we tune  $\alpha$  around  $\alpha = 1$ . The decreasing behavior of  $\xi_N^{(3)}$  disappears around  $\alpha = 1.2$ ; however,  $\xi_N^{(4)}$  is still decreasing. The present examination of data up to  $N = 24$  suggests that it becomes unclear whether  $A_{N=22}^{(5)} = 0.410498$  is appropriate as a reliable estimate or not according to the criteria of the above three conditions. At least for  $\alpha = 1$ , the acceleration of  $A_N^{(k)}$  up to  $k = 2$  seems to be successful. It is possible to use  $A_N^{(2)}$  instead of  $A_{N=22}^{(5)}$  as a reliable estimate. In this case, let us remember that  $A_N^{(2)}$  is monotonically decreasing. This suggests that any of data in  $A_N^{(2)}$  gives an upper bound for the true Haldane gap. Even though the value of  $\alpha$  is tuned, one obtains only an assembly of upper bounds. There is no evidence to show that the true gap value is in the region of the assembly. Thus, tuning  $\alpha$  is not an appropriate way to obtain a reliable error of the Haldane gap. Therefore, we have to develop another strategy without tuning  $\alpha$  to achieve it.

Next, we present the result of the convergence acceleration of our gap data under the twisted boundary condition. The table for  $\alpha = 1$  is shown in Table II. One can observe that all the above conditions hold. It is reasonable to consider that all of  $A_N^{(k)}$  are successfully accelerated. The difference between the periodic and twisted boundary conditions is the direction of  $A_N^{(k)}$ ; namely  $A_N^{(k)}$  in Table II is monotonically increasing. This means that the data in  $A_N^{(k)}$  are lower bounds. In order to obtain a reliable error only from the data under the twisted boundary condition, it is required to create another sequence that is monotonically decreasing. Here let us consider a

new sequence defined as

$$B_{N+1}^{(k)} = \frac{T_N S_{N+2} - T_{N+2} S_N}{S_{N+2} - S_N - T_{N+2} + T_N}, \quad (10)$$

where  $T_N = A_N^{(k)}$  and  $S_N = A_N^{(k-1)}$ . If  $A_N^{(k)}$  is successfully accelerated from  $A_N^{(k-1)}$ , it is expected that the sequence  $B_{N+1}^{(k)}$  is convergent from the side opposite to  $T_N = A_N^{(k)}$  and  $S_N = A_N^{(k-1)}$ . (See appendix.) In Table III, we present the result of  $B_N^{(k)}$  obtained from  $A_N^{(k)}$  under the twisted boundary condition. One observes that all of  $B_N^{(k)}$  are decreasing with increasing  $N$ . The difference of the dependences of  $A_N^{(k)}$  and  $B_N^{(k)}$  makes us know that the true gap value is between them. In this works, we employ  $A_N^{(4)}$  and  $B_N^{(4)}$  whose dependences are confirmed to be opposite to play safe. Namely, the  $S = 1$  Haldane gap is expected to be between  $A_{N=24}^{(4)} = 0.41047777$  and  $B_{N=23}^{(4)} = 0.41048023$ . Therefore, our present consequence for the Haldane gap for  $S = 1$  is

$$0.4104789 \pm 0.0000013. \quad (11)$$

This estimate agrees with the estimate from the QMC method<sup>6</sup> and that from the DMRG one.<sup>5</sup> Note that our estimate (11) is more precise than any other estimates as long as the present authors know. Before finishing this paragraph, we illustrate  $A_N^{(k)}$  and  $B_N^{(k)}$  in Fig. 3 so that one visually captures the features of these sequences, which are explained in the above.

The sequence  $B_N^{(k)}$  is a general way to estimate a reliable error; the case of the periodic boundary condition in Table I is applicable. In this case,  $B_N^{(k)}$  is created from  $S_N = A_N^{(1)}$  and  $T_N = A_N^{(2)}$  because it is confirmed that  $A_N^{(2)}$  is successfully accelerated from  $A_N^{(1)}$ . Note that in this case,  $B_N^{(k)}$  is monotonically increasing and converging from the smaller side. Thus,  $B_N^{(k)}$  gives a lower bound of the gap value. The data up to  $N = 24$  under the periodic boundary condition suggests that the Haldane gap is between  $B_{N=23}^{(2)}$  and  $A_{N=24}^{(2)}$ ; we have  $0.41050 \pm 0.00005$  as an estimate in the periodic boundary condition. This result is also consistent with the estimate (11), the one from the QMC method,<sup>6</sup> and the one from the DMRG one.<sup>5</sup> This indicates that the present procedure makes it

Table II. Sequence of finite-size gaps for the  $S = 1$  case under the twisted boundary condition and the convergence acceleration based on Wynn's algorithm (eq.(6) with  $\alpha = 1$ ).

$N$	$G(N) = A_N^{(0)}$	$\xi_N^{(0)}$	$A_N^{(1)}$	$\xi_N^{(1)}$	$A_N^{(2)}$	$\xi_N^{(2)}$	$A_N^{(3)}$	$\xi_N^{(3)}$	$A_N^{(4)}$	$\xi_N^{(4)}$	$A_N^{(5)}$
4	0.297769379131										
6	0.362613495315										
8	0.386237672978	1.98	0.39977728								
10	0.396943190982	2.53	0.40581471								
12	0.402443823536	3.00	0.40825701	2.21	0.40920572						
14	0.405509288158	3.42	0.40936819	2.54	0.40998448						
16	0.407315632794	3.78	0.40990703	2.76	0.41027702	2.04	0.41035307				
18	0.408423139414	4.09	0.41017830	2.91	0.41039295	2.16	0.41043554				
20	0.409122144092	4.35	0.41031824	3.02	0.41044086	2.26	0.41046285	1.81	0.41046801		
22	0.409572951736	4.56	0.41039177	3.11	0.41046146	2.37	0.41047263	1.95	0.41047535		
24	0.409868488828	4.74	0.41043100	3.18	0.41047068	2.49	0.41047640	2.10	0.41047777	1.80	0.41047815

Table III. Upper-bound sequence  $B_N^{(k)}$  of the  $S = 1$  Haldane gap.

$N$	$B_N^{(1)}$	$B_N^{(2)}$	$B_N^{(3)}$	$B_N^{(4)}$
9	0.41728860			
11	0.41289925			
13	0.41156232	0.41142826		
15	0.41100869	0.41071649		
17	0.41074765	0.41055312	0.41054058	
19	0.41061764	0.41050468	0.41049203	
21	0.41055134	0.41048859	0.41048271	0.41048358
23	0.41051712	0.41048286	0.41048036	0.41048023

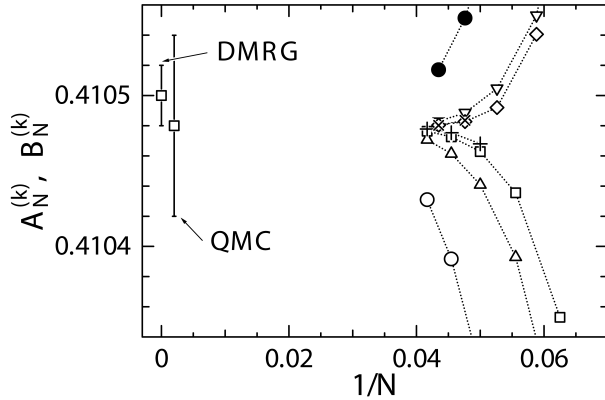


Fig. 3. The system size dependence of the sequences  $A_N^{(k)}$  and  $B_N^{(k)}$  under the twisted boundary condition. Open circles, triangles, squares, pluses denote  $A_N^{(1)}$ ,  $A_N^{(2)}$ ,  $A_N^{(3)}$ , and  $A_N^{(4)}$ , respectively. Closed circles, reversed triangles, diamonds, crosses denote  $B_N^{(1)}$ ,  $B_N^{(2)}$ ,  $B_N^{(3)}$ , and  $B_N^{(4)}$ , respectively. The estimates of the  $S = 1$  gap from the QMC method<sup>6</sup> and from the DMRG one<sup>5</sup> are also presented near the left-hand ordinate.

possible to estimate the gap value irrespective of boundary conditions. The difference of systematic errors between the cases of the periodic boundary condition and the twisted boundary condition originates from the characteristics of the initial sequences. In this meaning, the twisted boundary condition is better than the periodic boundary condition to estimate the Haldane gap.

### 3.2 Cases for $S \geq 2$

In this subsection, we estimate the Haldane gap for  $S \geq 2$ . We employ the twisted boundary condition to obtain the finite-size gap  $G(N)$ . Since the sequence  $G(N)$

is increasing with  $N$ , it is easy to distinguish whether the gap survives or not in the limit of  $N \rightarrow \infty$  even though the gap value is extremely small.

Let us extrapolate our finite-size gaps for the  $S = 2$  case by eqs. (6) and (10). The result is summarized in Table IV. One finds that data for small  $N$  disturb the table. In Table IV,  $A_4^{(0)}$  and data originating from it are underlined. If we exclude these underlined data from the table, all other data do not disturb the table, which suggests that the convergence acceleration of the sequence  $A_N^{(0)}$  starting from  $N = 6$  is successful. One can also find that  $B_N^{(1)}$  without the underline show the dependence opposite to  $A_N^{(k)}$ . After excluding the underlined data, we do not have a sufficient number of data in  $B_N^{(2)}$  to know its dependence; thus, we do not employ  $B_{15}^{(2)}$  as an upper bound in this work. In addition, we cannot confirm whether  $A_{14}^{(2)}$  and  $A_{16}^{(2)}$  are successfully accelerated or not, because available  $\xi_N^{(2)}$  originates from  $A_4^{(0)}$ . From the above reason, it is a careful and reliable judgment to consider that  $\Delta(S = 2)$  is between  $A_{16}^{(1)}$  and  $B_{15}^{(1)}$ . Therefore our conclusion of the estimates for  $\Delta(S = 2)$  is

$$0.0886 \pm 0.0018, \quad (12)$$

for  $S = 2$ . This estimate agrees with  $\Delta = 0.08917 \pm 0.00004$  from the QMC simulation in ref. 6 and  $\Delta = 0.0876 \pm 0.0013$  from the DMRG calculation in ref. 12.

Next, we study the cases for  $S \geq 3$ . Our numerical results under the twisted boundary condition are presented in Table V. One can observe that the decay length in  $S = 4$  and 5 is not monotonically increasing. Although the decay length  $\xi_N^{(0)}$  in  $S = 3$  is monotonically increasing,  $\xi_N^{(1)}$  is negative. This indicates that  $A_4^{(0)}$  and its posterity should be excluded from the table of acceleration according to the above criteria used in the case of  $S = 2$ . After the exclusion, one cannot judge whether  $A_N^{(1)}$  is successfully accelerated within the present data. Thus, we do not apply the above acceleration procedure to these finite-size gaps of  $S \geq 3$  in this study.

For  $S \geq 3$ , a serious behavior of the finite-size deviations appears when one draws a plot of  $G(N)$  versus the inverse of the system size as a way that is usually applied. In this plot, the  $1/N$ -dependence of  $G(N)$  reveals concave upwards for small sizes. For  $S = 3$  and

Table IV. Sequence of finite-size gaps for the  $S = 2$  case under the twisted boundary condition, the convergence acceleration based on Wynn's algorithm, and upper-bound sequence  $B_N^{(k)}$ .

$N$	$10^2 A_N^{(0)}$	$\xi_N^{(0)}$	$10^2 A_N^{(1)}$	$\xi_N^{(1)}$	$10^2 B_N^{(1)}$	$10^2 A_N^{(2)}$	$\xi_N^{(2)}$	$10^2 B_N^{(2)}$
4	<u>3.60543243815</u>							
6	5.88636574630							
8	6.98099292140	<u>2.72</u>	<u>7.9910262</u>					
9					<u>9.046111</u>			
10	7.57841496301	3.30	8.2962537					
11					9.125346			
12	7.93926067768	3.97	8.4896523	<u>4.38</u>		<u>8.6729401</u>		
13					9.068141			<u>8.814100</u>
14	8.17386831221	4.65	8.6098758	4.21		8.7252465		
15					9.021915			8.963622
16	8.33497991928	5.32	8.6881548	4.66		8.7779957	<u>-237.32</u>	

Table V. Finite-size gaps and decay lengths for the  $S \geq 3$  cases under the twisted boundary condition. For  $S = 3$ , the convergence acceleration based on Wynn's algorithm is also applied.

$N$	$S = 3$				$S = 4$		$S = 5$	
	$10^3 A_N^{(0)}$	$\xi_N^{(0)}$	$10^3 A_N^{(1)}$	$\xi_N^{(1)}$	$10^4 A_N^{(0)}$	$\xi_N^{(0)}$	$10^5 A_N^{(0)}$	$\xi_N^{(0)}$
4	2.44233786473				1.29166071630		0.59777444079	
6	5.20317763910				3.52085939468		2.06995173926	
8	6.75739139783	3.48	8.75932105666		4.94293026662	4.45	3.12913003881	6.07
10	7.66279200087	3.70	8.92625320663		5.80259274045	3.97	3.79423190111	4.30
12	8.23027668731	4.28	9.18329148633	-4.63	6.34716007738	4.38		

4, the dependence becomes convex upwards for larger sizes. For  $S = 5$ , the dependence is still concave upwards in the range up to  $N = 10$ . If the dependence is concave upwards, it is difficult for us to capture a converging behavior.

Under these circumstances, we take a strategy composed of the following two steps. The first step is to draw a plot of  $G(N)$  so that a shape which is concave upwards does not appear. The second step is to create a decreasing sequence from  $G(N)$  that is an increasing sequence in the new plot.

In order to carry out the first step, we here introduce a renormalized system size  $\tilde{N}$  defined as  $N + N_0$  so that three data for  $N = 4, 6$ , and  $8$  reveal a linear dependence in the plot of  $G(N)$  versus  $1/\tilde{N}$ . The results are depicted in Fig. 4. One can observe the  $1/\tilde{N}$ -dependence of  $G(N)$  is always convex upwards in every  $S$  of Fig. 4 (a)-(d). Note in Fig. 4 (a) and (b) that  $G(N)$  approaches an estimate obtained from QMC in ref. (6) for  $S = 2$  and  $3$ . On the other hand, we do not have other estimates with which we can compare our  $G(N)$  for  $S = 4$  and  $5$ . All of  $G(N)$  in Fig. 4 are increasing with  $N$ . Thus, our finite-size gaps  $G(N)$  under the twisted boundary condition are appropriate to estimate the Haldane gaps even for  $S \geq 2$ . One finds that  $G(N)$  gives lower bounds for the Haldane gaps.

Next, we perform the second step. We focus on neighboring three data points of system sizes  $N-2$ ,  $N$ , and  $N+2$  in each panel of Fig. 4. When we apply the fitting curve of

$$y = C + Dx^E, \quad (13)$$

to the three data points, it is possible to determine the parameters  $C$ ,  $D$ , and  $E$  uniquely for a given  $N$ . Then we use  $C(N)$ ,  $D(N)$ , and  $E(N)$  hereafter. Due to the

above first step,  $E(N = 6)$  is necessarily the unity. Note that  $D(N)$  is monotonically decreasing with increasing  $N$  and that  $E(N)$  is monotonically increasing. The result of  $C(N)$  are also depicted at the corresponding  $\tilde{N}$  in Fig. 4. One can observe that  $C(N)$  is monotonically decreasing with increasing  $N$  in Fig. 4 (a)-(d). At least for  $S = 2$  and  $3$ ,  $C(N)$  seems to converge from the upper side to the gap value estimated from QMC calculations.<sup>6</sup> It is reasonable to consider that the sequence  $C(N)$  becomes an upper bound of the gap value. We choose  $C(N)$  for the largest system sizes as the best upper bound in the analysis of Fig. 4 (a)-(d). From the above argument of the lower and upper bounds of the gap value, we obtain

$$\Delta(S = 2) = 0.0868 \pm 0.0034, \quad (14)$$

$$\Delta(S = 3) = 0.0092 \pm 0.0010, \quad (15)$$

$$\Delta(S = 4) = 0.00072 \pm 0.00009, \quad (16)$$

$$\Delta(S = 5) = 0.000047 \pm 0.000010. \quad (17)$$

The estimate (14) for  $S = 2$  is consistent with the above result (12). We can also compare our estimate of  $\Delta(S = 3)$ ; our estimate agrees with  $\Delta = 0.01002 \pm 0.00003$  from the QMC simulation in ref. 6. There is no other numerical estimate for  $S \geq 4$  to the best of our knowledge. Our estimate (16) and (17) will be inspected in future if other methods become available.

Note here that the analysis without convergence acceleration is also applicable to the case of  $S = 1$ ; the result is

$$\Delta(S = 1) = 0.41028 \pm 0.0042. \quad (18)$$

This estimate is consistent with the gap (11). One of the differences is that the error of (18) is wider than the one of (11). The same situation appears between (14) and

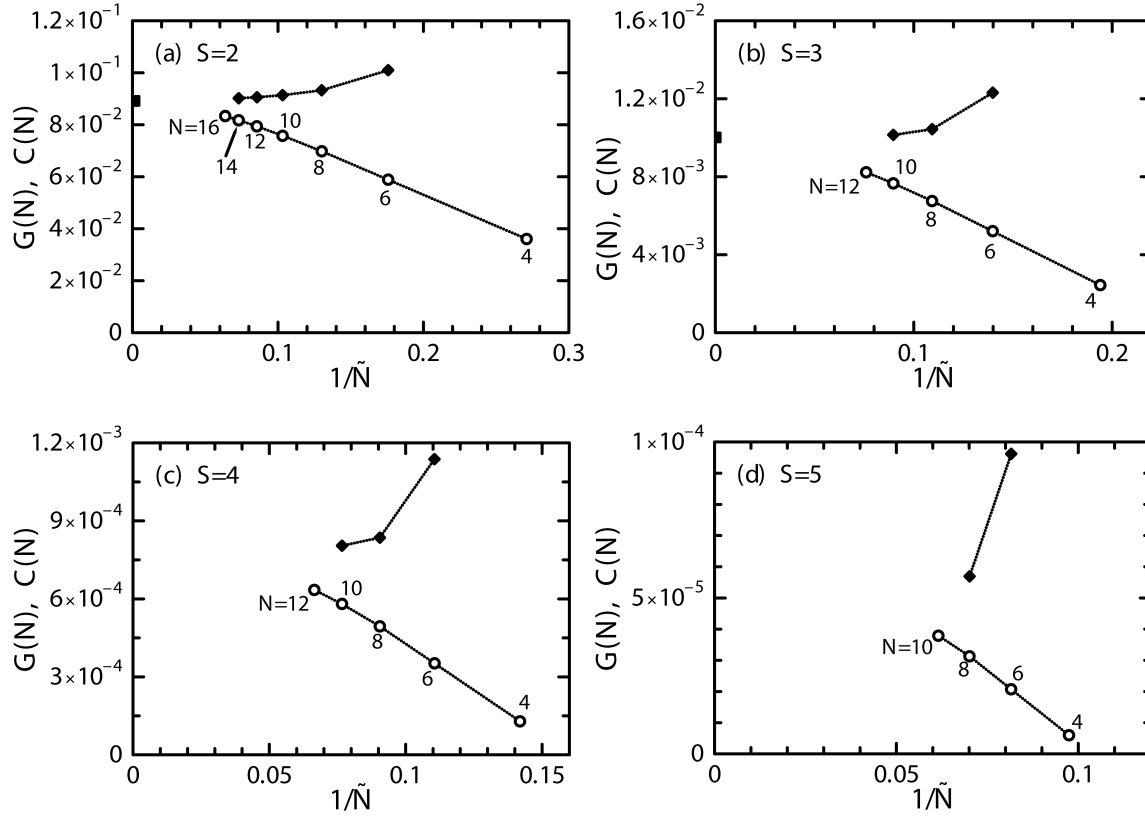


Fig. 4. Finite-size gaps  $G(N)$  for  $S = 2, 3, 4,$  and  $5$  under the twisted boundary condition are shown by open circles. We determine a renormalized system size  $\tilde{N}$  defined as  $N + N_0$  so that three data for  $N = 4, 6,$  and  $8$  reveal a linear dependence;  $N_0 = -0.3091268, 1.15226211, 3.04756114,$  and  $6.25840221$  for  $S = 2, 3, 4,$  and  $5,$  respectively. For  $S = 2$  and  $3,$  the results from QMC in ref. (6) are shown by closed squares. Diamonds represent upper bounds  $C(N)$ . Equation (13) gives  $C(N)$  from the finite-size gaps of system sizes  $N-2, N,$  and  $N+2$ .

(12) in the case of  $S = 2$ . These agreements for  $S = 1$  and  $2$  suggest that both the methods successfully lead to the common estimate that is irrespective of analyzing methods. Another difference is that the central value of the estimate (18) is slightly smaller than that of the estimate (11). One can also in the case of  $S = 2$  observe that the central value of the estimate (14) is smaller than that of the estimate (12). The estimate from the QMC simulation in ref. 6 is larger than the central value of the estimate (15) in the case of  $S = 3$ . These facts suggest that the present method using eq. (13) may give us the central value that is closer to the data of the original sequence. One of the reason may be that  $C(N)$  of eq. (13) is closer to the true quantity in the thermodynamic limit because  $C(N)$  is a kind of extrapolated results. It is not so easy to know where within the error the true infinite-size quantity is only from the data of this work without referring other information. However, this question is beyond the present study because a primary purpose of this work is the development of a method that makes us possible to obtain a reliable systematic error within which there exists the true infinite-size quantity.

Here, we examine the asymptotic formula of the Haldane gap,

$$\Delta(S) = \beta |\mathbf{S}|^2 \exp(-\pi |\mathbf{S}|), \quad (19)$$

for  $S \rightarrow \infty$  from our estimate of the gaps for finite  $S$ . In order to do it, we introduce new parameters  $x = S^{-1}$

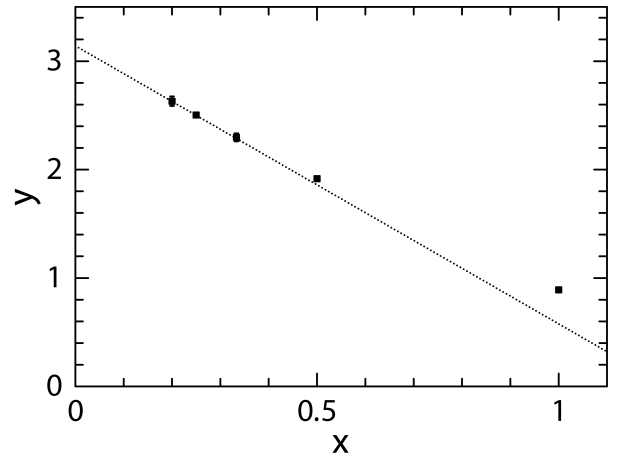


Fig. 5. Analysis of our estimates of Haldane gaps up to  $S = 5$  to confirm the asymptotic formula for large  $S$ . Errors for  $S = 1$  and  $2$  are smaller than the symbol size. The dotted line is the one with  $\beta \sim 12.8$  obtained from the linear fitting of  $S = 4$  and  $5$ .

and  $y = S^{-1} \log(S^2/\Delta(S))$  when we take the amplitude of each spin to be  $|\mathbf{S}| = S$  in the present analysis.<sup>13</sup> The asymptotic formula (19) is rewritten as

$$y = \pi - x \log \beta. \quad (20)$$

Let us input our estimates of the Haldane gaps to  $\Delta(S)$  in  $y$  and plot the  $x$  dependence of  $y$ . The result is depicted

in Fig. 5. One can find a linear behavior for finite but large  $S$  up to  $S = 5$ . We have fitted our data for  $S = 4$  and 5 with the straight line (20); the best fit is produced by  $\beta = 12.8 \pm 1.5$ . The linear behavior suggests that the asymptotic formula (19) holds well for large  $S$ . Note here that if one uses the formula (19) and our estimate of  $\beta$ , one can predict the magnitude of the Haldane gap for  $S > 5$ .

#### 4. Summary and Remarks

We have developed methods to estimate a systematic error in the extrapolation of finite-size data obtained from numerical diagonalizations of small clusters. The methods have been applied to study the Haldane gaps of the one-dimensional integer- $S$  Heisenberg antiferromagnet. We have demonstrated that the methods work well to the finite-size data under the twisted boundary condition. Our best estimate of the  $S = 1$  case is  $\Delta = 0.4104789 \pm 0.0000013$ . We are also successful in obtaining the gaps up to  $S = 5$  even though the magnitudes of the gaps are extremely small. Our estimates of the gaps for large  $S$  make us confirm that the asymptotic formula of the gap holds well. We have found that the twisted boundary condition is more appropriate than the periodic and open boundary conditions in order to extrapolate finite-size data of the Haldane gaps to the thermodynamic limit. However, the most appropriate boundary condition is not always the twisted boundary condition. The most appropriate boundary condition depends on the model and physical quantities.<sup>14</sup> The present work strongly suggests that the examination of various boundary conditions is useful to know reliable quantities in the thermodynamic limit. It should be examined in future studies whether the methods work or not in extrapolations of other quantities, like the correlation functions of a system. The present method could give detailed information about the quantum state, which contributes much to a deeper understanding of properties of the system.

Finally, it is noticeable that to produce a new sequence by eq.(10) is a quite versatile way. Only Wynn's transformation is employed in this work, but eq.(10) is available irrespective of acceleration methods. The parameter of sequences is not limited to the system size. Usefulness of this way for other parameters should be examined. In principle, the way of  $B_N^{(k)}$  is applicable when the number of data in an original sequence  $A_N^{(0)}$  is five at least because the direction of the dependence of  $B_N^{(k)}$  can be checked. Note also that properties of the new sequence  $B_N^{(k)}$  are related to whether the acceleration procedure is successful or not as we have mentioned in Appendix.

#### Acknowledgment

We wish to thank Prof. K. Hida, Dr. K. Okamoto, Prof. T. Sakai, Prof. K. Kusakabe, and Dr. S. Todo for fruitful discussions. This work was partly supported by Grants-in-Aid from the Ministry of Education, Culture, Sports, Science and Technology (No. 20340096). A part of the computations was performed using facilities of the Information Initiative Center, Hokkaido University

and the Supercomputer Center, Institute for Solid State Physics, University of Tokyo.

#### Appendix: Convergence acceleration and new sequence

Let us consider monotonic scalar sequences  $T_n$  and  $S_n$  that share the common limit  $S$ . According to ref. 17, the convergence of  $T_n$  is faster than that of  $S_n$  when the following condition is satisfied

$$\lim_{n \rightarrow \infty} \frac{T_n - S}{S_n - S} = 0. \quad (\text{A}\cdot 1)$$

In a practical problem, however, lengths of the sequences are finite;  $S$  is not a known quantity but the one that should be obtained. Therefore, the condition (A.1) cannot be examined directly. A substitute condition for (A.1) is given by

$$\lim_{n \rightarrow \infty} \frac{T_n - T_{n+m}}{S_n - S_{n+m}} = 0. \quad (\text{A}\cdot 2)$$

for an arbitrary integer  $m(> 0)$ . eq. (A.2) suggests that

$$\begin{aligned} 1 &> \left| \frac{T_n - T_{n+m}}{S_n - S_{n+m}} \right| \\ &> \left| \frac{T_{n+\delta n} - T_{n+\delta n+m}}{S_{n+\delta n} - S_{n+\delta n+m}} \right| \\ &> \left| \frac{T_{n+2\delta n} - T_{n+2\delta n+m}}{S_{n+2\delta n} - S_{n+2\delta n+m}} \right| > \dots, \end{aligned} \quad (\text{A}\cdot 3)$$

for  $n$  in the region where a converging behavior appears in  $(T_n - T_{n+m})/(S_n - S_{n+m})$ . Note here that this equation with  $\delta n = m = 2$  is related to eq. (9).

Let us get back to eq. (A.1). Suppose that both  $S_n$  and  $T_n$  approach  $S$  from the same side. The equation (A.1) suggests that

$$\frac{T_{n+m} - S}{S_{n+m} - S} < \frac{T_n - S}{S_n - S}, \quad (\text{A}\cdot 4)$$

for sufficiently large  $n$  and positive  $m$ . This inequality is rewritten as

$$[(S_{n+m} - S_n) - (T_{n+m} - T_n)]S < T_n S_{n+m} - T_{n+m} S_n, \quad (\text{A}\cdot 5)$$

because  $S_n$  is monotonic. When  $T_n$  is obtained from  $S_n$  through a successful acceleration procedure and when  $S_n$  and  $T_n$  are monotonically increasing, one can find

$$S < \frac{T_n S_{n+m} - T_{n+m} S_n}{(S_{n+m} - S_n) - (T_{n+m} - T_n)}. \quad (\text{A}\cdot 6)$$

The right hand side of this inequality can be written to be

$$S + \frac{T_n - S - \frac{T_{n+m} - T_n}{S_{n+m} - S_n} (S_n - S)}{1 - \frac{T_{n+m} - T_n}{S_{n+m} - S_n}}, \quad (\text{A}\cdot 7)$$

which is easily found to converge to  $S$  in the limit of  $n \rightarrow \infty$  with a help of the limit (A.2).

Let us consider the case of  $T_n = A_n^{(k)}$ ,  $S_n = A_n^{(k-1)}$ , and  $m = 2$ ; The right hand side of the inequality (A.6) becomes  $B_{n+1}^{(k)}$ . From the inequality (A.6) and the limit of (A.7),  $B_{n+1}^{(k)}$  defined as eq. (10) is found to converge to  $S$  from the upper side. Note that the direction of the



Table A.1. An application of the convergence acceleration to the sequence (A.8) having its limit as  $\pi$ . The decay lengths obtained from each sequence by eq. (7) are also accompanied.

$N$	$A_N^{(0)}$	$\xi_N^{(0)}$	$A_N^{(1)}$	$\xi_N^{(1)}$	$A_N^{(2)}$	$\xi_N^{(2)}$	$A_N^{(3)}$	$\xi_N^{(3)}$	$A_N^{(4)}$	$\xi_N^{(4)}$	$A_N^{(5)}$
2	2.922835737772										
4	3.032442077939										
6	3.081373479799	2.48	3.12083429								
8	3.106348882832	2.97	3.13238707								
10	3.120142116779	3.37	3.13715611	2.26	3.13939334						
12	3.128166065374	3.69	3.13932581	2.54	3.14068137						
14	3.133009091490	3.96	3.14038271	2.78	3.14118662	2.14	3.14135408				
16	3.136013726258	4.19	3.14092445	2.99	3.14140146	2.34	3.14149788				
18	3.137917979434	4.39	3.14121336	3.18	3.14149861	2.52	3.14155251	2.07	3.14156654		
20	3.139145542642	4.56	3.14137243	3.35	3.14154473	2.68	3.14157476	2.23	3.14158257		
22	3.139947946854	4.70	3.14146233	3.50	3.14156750	2.83	3.14158434	2.37	3.14158853	2.02	3.14158978

convergence of  $B_{n+1}^{(k)}$  is opposite to that of  $T_n$  and that of  $S_n$ .

The above argument is applicable when  $S_n$  and  $T_n$  are monotonically decreasing. In this case,  $B_{n+1}^{(k)}$  converges to  $S$  from the lower side. The direction of the convergence of  $B_{n+1}^{(k)}$  is opposite to that of  $T_n$  and that of  $S_n$  irrespective of the direction of  $T_n$  and  $S_n$ .

Finally, a numerical example is presented for a demonstration of the procedure proposed in this paper. We consider the sequence  $\{A_N^{(0)}\} = \{A_2^{(0)}, A_4^{(0)}, A_6^{(0)}, A_8^{(0)}, \dots\}$  defined as

$$A_N^{(0)} = \sum_{k=0}^{N/2} \frac{(2k-1)!!}{(2k)!!} \frac{3}{2k+1} \left(\frac{\sqrt{3}}{2}\right)^{2k+1}, \quad (\text{A.8})$$

where  $(2k)!! = (2k)(2k-2)\dots 4 \cdot 2$  and  $(2k-1)!! = (2k-1)(2k-3)\dots 3 \cdot 1$ . This initial sequence is obvious to increase monotonically. It is easily understood that the limit of  $N \rightarrow \infty$  is given by  $3 \arcsin(\sqrt{3}/2) = \pi (= 3.14159265\dots)$  if one remembers the Taylor expansion of  $\arcsin x$  in a neighborhood of  $x = 0$ . If we apply Wynn's transformation (6) and create a new sequence  $B_{n+1}^{(k)}$  by means of eq. (10) in the case of  $T_N = A_N^{(k)}$  and  $S_N = A_N^{(k-1)}$ . The result is summarized in Table A.1, Table A.2, and Fig. A.1. One can confirm a successful acceleration of convergence of  $A_N^{(k)}$  in Table A.1 from a judgement based on Conditions **I**, **II**, and **III** in §3.1.2. A successful creation of  $B_N^{(k)}$  which decreases monotonically with respect to  $N$  can be observed in Table A.2. Figure A.1 is presented in order to confirm that the features of  $A_N^{(k)}$  and  $B_N^{(k)}$  hold for even larger  $N$ . One can find that each  $B_N^{(k)}$  approaches the exact value from the upper side while  $A_N^{(k)}$  approaches it from the opposite, namely lower, side. It is reasonable to consider that each datum of  $A_N^{(k)}$  and  $B_N^{(k)}$  is a lower bound and an upper bound, respectively, for the rigorous limit  $\pi$ .

- 1) F. D. Haldane: Phys. Rev. Lett. **50** (1983) 1153.
- 2) F. D. Haldane: Phys. Lett. **93A** (1983) 464.
- 3) Various estimates of the Haldane gap of  $S = 1$  chain was extensively summarized in ref. 4. The case of  $S = 2$  was given in Table I of ref. 12.
- 4) O. Golinelli, T. Jolicœur, and R. Lacaze: Phys. Rev. B **50** (1994) 3037.
- 5) S. R. White and D. A. Huse: Phys. Rev. B **48** (1993) 3844.

- 6) S. Todo and K. Kato: Phys. Rev. Lett. **87** (2001) 047203.
- 7) A. Terai: presented at 19th IUPAP Int. Conf. Stat. Physics, 1995
- 8) When system sizes are very small, the dimensions of the Hilbert space are also small; Lanczos calculations sometimes become unstable. In these cases, we perform the Householder diagonalizations instead.
- 9) P. Wynn: Numer. Math. **8** (1966) 264.
- 10) D. Shanks: J. Math. Phys. (Cambridge, Mass.) **34** (1955) 1.
- 11) T. Sakai and M. Takahashi: Phys. Rev. B **42** (1990) 1090.
- 12) X. Wang, S. Qin, and L. Yu: Phys. Rev. B **60** (1999) 14529.
- 13) Another possibility is  $|\mathbf{S}| = \sqrt{S(S+1)}$ . When we use  $x = 1/\sqrt{S(S+1)}$  and  $y = [S(S+1)]^{-1/2} \log(S(S+1)/\Delta(S))$  in this case, the analysis based on the same linear line (20) is available.

Table A.2. Upper-bound sequence  $B_N^{(k)}$  calculated with eq. (10) from  $A_N^{(k)}$  in Table A.1.

$N$	$B_N^{(1)}$	$B_N^{(2)}$	$B_N^{(3)}$	$B_N^{(4)}$
7	3.15479800			
9	3.14614753			
11	3.14346184	3.14266173		
13	3.14244105	3.14192290		
15	3.14200462	3.14171496	3.14169304	
17	3.14180277	3.14164312	3.14162175	
19	3.14170394	3.14161507	3.14160274	3.14160271
21	3.14165340	3.14160317	3.14159655	3.14159545

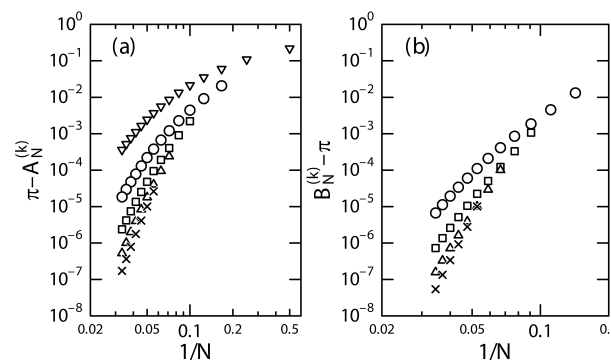


Fig. A.1. Log-log plots of (a)  $\pi - A_N^{(k)}$  and (b)  $B_N^{(k)} - \pi$  of sequence (A.8) for  $N$  up to 30. Reversed triangles, circles, squares, triangles, and crosses in (a) denote  $\pi - A_N^{(0)}$ ,  $\pi - A_N^{(1)}$ ,  $\pi - A_N^{(2)}$ ,  $\pi - A_N^{(3)}$ , and  $\pi - A_N^{(4)}$ , respectively. Circles, squares, triangles, and crosses in (b) denote  $B_N^{(1)} - \pi$ ,  $B_N^{(2)} - \pi$ ,  $B_N^{(3)} - \pi$ , and  $B_N^{(4)} - \pi$ , respectively.

- 14) An example of a different model was reported in refs. 15 and 16.
- 15) H. Nakano and Y. Takahashi: J. Phys. Soc. Jpn. **73** (2004) 983.
- 16) H. Nakano, Y. Takahashi, and M. Imada: J. Phys. Soc. Jpn. **76** (2007) 034705.
- 17) C. Brezinski: J. Comp. Appl. Math. **122** (2000) 1.